Preparation and electrochemical characterization of PANI/PVA and PANI/Zr/PVA composites for supercapacitor application

Tatiana N. Myasoedova[1*], Eugeniya N. Shishlyanikova[1], Tatiana A. Moiseeva[1], Maria Brzhezinskaya[2]

[1]*Department of Technospher Safety and Chemistry, Southern Federal University, Chekhov str. 2, Taganrog 347928, Russia*
[2]*Institute of Nanometer Optic and Technology, Albert-Einstein-Str. 1512489 Berlin, Germany*

[*]Corresponding author. Tel: (+7) 8634371624; E-mail: tnmyasoedova@sfedu.ru

ABSTRACT

In the present work, the PANI and PANI/Zr composite powders were synthesized by the method of chemical polymerization in the inorganic acid medium. The morphology of prepared composites demonstrates fiber-like structure revealed by scanning electron microscopy. The value of the specific surface area estimated by the BET technique depends on the type of the composite powder and was found to be 66.8 and 142.05 m^2/g for PANI and PANI/Zr respectively. UV–Vis spectroscopy was employed to characterize the optical properties of the synthesized powder composites. The incorporation of zirconium gives rise to the red shift of π– π* transition of pristine PANI. The synthesized composite powders were used for preparation of PANI/PVA and PANI/Zr/PVA composites which electrochemical properties were compared in different electrolytes: 0.5 M KOH, 0.5 M NaCl and 0.5 M H_2SO_4. Excellent electrochemical reversibility was found out for both PANI/PVA and PANI/Zr/PVA composites. Effect of electrolyte type and current value on the specific capacitance of the prepared composites was observed. Copyright © 2016 VBRI Press.

Keywords: Polyaniline; polyvinyl alcohol; zirconium; specific capacitance.

Introduction

Conductive polymers, such as polyaniline (PANI), polyacrilonitrile and polypyrrole, have been the subject of numerous investigations in the past two decades for electronics application.

Conductive polymers are applicable for light emitting diodes (LEDs), corrosion resistance coatings [1], electromagnetic shielding [2, 3], sensor technology [4, 5], medicine [6], molecular electronics [4, 5], superpercapacitors, and electrochromic devices [7]. By judiciously choiring the molecule combinations, it is possible to prepare multifunctional molecular structures that open possibilities for almost any desired applications.

The inorganic-organic composite materials are increasingly significant due to the extraordinary properties. Such components as metals and their oxides ensured to enhance thermal and chemical stability of the polymer itself as well as to increase the specific surface area. [10 - 13]. Polymer matrix provides the process ability and flexibility and at the same time the inorganic particles not only improve the mechanical properties of the host polymer, but also give unique properties which differ from their bulk materials and atoms [8]. PANI is a particularly interesting conducting polymer has attracted intense interest due to its environmental stability, facile synthesis (it can be easily prepared by both chemical and electro-chemical routes), and exciting electrochemical, optical and electrical properties [9].

The processability of PANI to make the films is rather difficult, because it is infusible and insoluble in common solvents. Also it attempts have been made to overcome these setbacks, for example, blending of PANI with other soluble polymers polyvinyl alcohol (PVA), polyethylene oxide, polymethyl methacrylate and etc. [14 -15]. PVA is bio-degradable synthetic polymer using as fiber, film, emulsifier, in the paper industry and etc.

A literature survey indicates that limited research studies on the preparation of PANI/PVA composites for supercapacitor application [16-18]. To the best of our knowledge, there has been no report on PVA–PANI–Zr composites. Zirconium and zirconium dioxide are thermally and chemically stable and good candidates for improving stability of polymer.

In this work, an attempt has been made to prepare PANI composites suitable for supercapacitor electrodes application.

Experimental

Preparation of PANI powder

Synthesis of PANI was described below. First, 1.57 mL of aniline was dissolved in 80 mL of 10 % HCl aqueous solution and the mixture was cooled to 0 °C. Then 16 ml of 1M $(NH_4)_2S_2O_8$ was dropwise into the above systems with a constant stirring, kept 30 minutes at 0 °C and then 60 min at room temperature. The product was filtered, and washed

with distilled water. After that, obtained wet powder was put into the flask with 15 % NH_4OH and kept for 48 hours. Finally, the product was filtered, washed with distilled water and dried at 80 °C until the constant weight.

Preparation of PANI/Zr powder

First, 0.81 g of $ZrOCl_2 \cdot 8H_2O$ was dissolved in 20 ml of distilled water and kept for 15 min. Then aniline solution in 10 % HCl (preparation is described in the section 2.1) was dropwise into zirconium solution. After that, 16 ml of 1M $(NH_4)_2S_2O_8$ was dropwise into the above systems with a constant stirring, kept 30 minutes at 0 °C and then 60 min at room temperature. The product was filtered, and washed with distilled water. The next step, obtained wet powder was put into the flask with 15 % NH_4OH and kept for 48 hours. Finally, the product was filtered, washed with distilled water and dried at 80 °C until the constant weight.

Preparation of PANI/PVA and PANI/Zr/PVA elastic electrodes

PVA was dissolved in distilled water in ration 1:9 with stirring for 20 min at 80 °C and, then cooled to room temperature. The next step, 0.65 g of the PANI or PANI/Zr powder was added into the 10 ml of PVA solution. The obtained mixture was continuously stirred for 10 min until a homogenous solution was obtained. After that, the as prepared mixture was poured into the Petri Dish and allowed to dry at 35 °C. The obtained polymer film was removed and cut into slices of 1x1 sm. The elastic electrodes for electrochemical performance were ready.
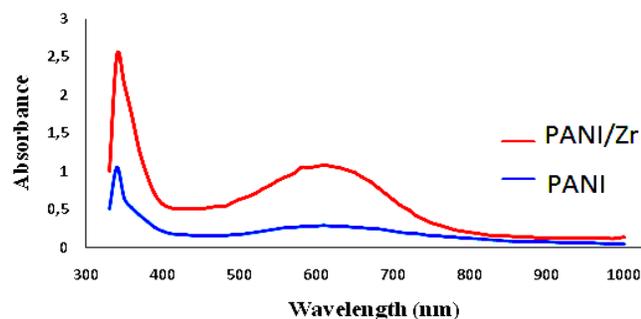

Fig. 1. UV–Vis spectra of pristine PANI and PANI/Zr composite

Instrumentation

The morphologies were observed by a scanning electron microscopy (LEO 1560 microscope). The PANI and PANI/Zr powders were dissolved in the dimethylformamide (DMFA) at 60°C and optic spectra were recorded by using a LEKISS1207 spectrometer. The Brunaer-Emmett- Teller (BET) specifiсe surface area, pore volume and pore size were investigated by an Asap 2020 surface area and pore size analyzer.

Electrochemical measurements

Cyclic voltammetry (CV) and galvanostatic charge/discharge measurements were recorded by an Ellins P-301 potentiostat at room temperature. The electrochemical cell was a conventional three-electrode cell. A commercial Ag/AgCl (3 M KCl) electrode was used as the reference electrode, and carbon electrode was used as the counter electrode. For CV measurements, the potential was scanned at 25, 50, 75, 100 mVs^{-1}. The charging–discharging measurement was made at different currents (0.5-3 mA). All characterizations were made in 0.5M KOH, 0.5M NaCl и 0.5 H_2SO_4 aqueous electrolytes.

Results and discussion

Characterization

UV–Vis spectroscopy was employed to characterize the optical properties of the synthesized powder composites. **Fig. 1** shows UV-Vis absorption spectra of the pure PANI, and PANI/Zr composite in DMFA solution. Two characteristic absorption bands are observed in the spectrum of pristine PANI and PANI/Zr composite at 320-340 nm and 580-620 nm wavelength, which attributed to π-π* conjugated ring and π-polaron benzenoid to quinoid excitonic transition, respectively. This result indicated that PANI is completely transformed from the emeraldine salt to the emeraldine base form. Furthermore, when zirconium particles are in the PANI matrix, a significant change is observed in the absorption spectrum. The red shift of the absorption transition to higher wavelength may be due to the successful interaction of zirconium particles with the polymer chain. The characteristic features of absorption spectrum indicate that PANI/Zr composite is in the conducting state.
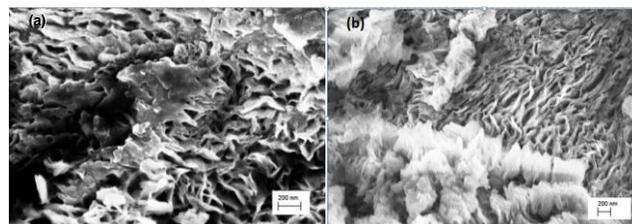

Fig. 2. SEM micrographs of PANI and PANI/Zr composite powders.

SEM micrographs show fiber-like structures of PANI and PANI/Zr with the average nanofibers diameter at the range of about 30-35 nm and 40-50 nm, respectively (**Fig. 2**). Increase of nanofiber diameter for PANI/Zr composite is observed comparing to pristine PANI. Also, the **Fig. 2b** performed the formation of a cotton-like structure as well as a fiber-like. This fact is explained by presence of zirconium containing particles effecting on the value of the specific surface area.

Isotherms of adsorption of PANI and PANI/ Zr powders were studied. The specific surface area of PANI determined by the BET method amounted to 66.8 m^2/g. The pore diameter varies from mesopores (2 nm) to macropores (160-170 nm) with the peak value falling on macropores and being 115 nm (**Fig. 2a**). The porous structure of PANI will be an added advantage for electron transfer when current is applied to the conductive polymer. The PANI/Zr surface area amounted to 146.05 m^2/g. The pore width made up 8 nm. Still, no distinct maximum can be observed when making a diagram of pore distribution by sizes

(**Fig. 3**), this rendering it difficult to estimate pore sizes by analyzing adsorption data (**Fig. 2b**).
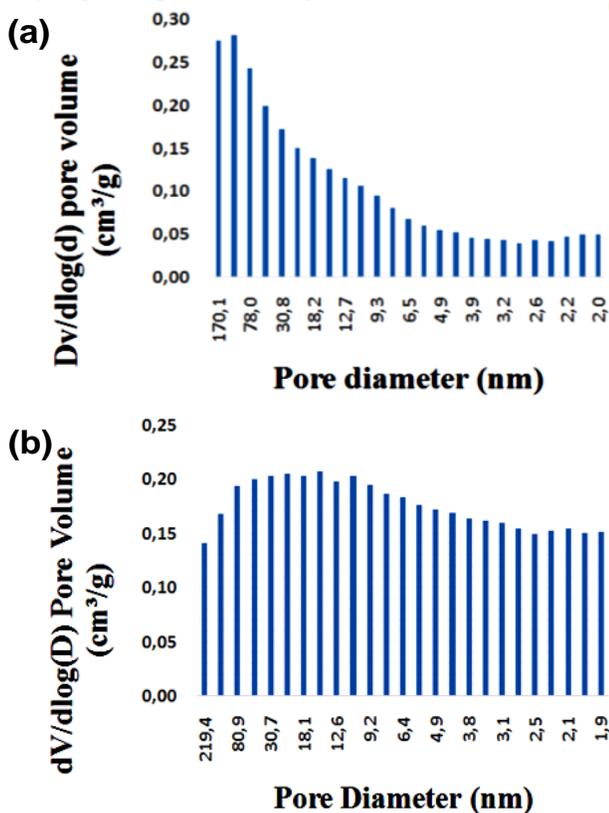

(a)

(b)

Fig. 3. Size-Volume Distribution of PANI (a) and PANI/Zr (b) Pore.

Electrochemical performance of PANI/PVA and PANI/Zr/PVA

The electrochemical characterization of the PANI/PVA composite is compared with PANI/Zr/PVA composite in **Fig. 4**. The potential-dependent processes of the two systems in different electrolytes are similar. CVs provide valuable information on charge-discharge behavior. Here, the capacitance was mainly based on the redox reaction because the shape of the CVs is distinguished from the shape of electric double-layer capacitance, which is normally close to an ideal rectangle. Electrochemical processes, including mixed electron-ionic controlled conductivity and redox-driven composition–structure relations proceed. Also, CVs curves exhibit two separate potential dependent redox responses, at the lower and extreme ends of the oxidation potentials. Mohamoud A.M. [19] suggests that this separation is due to the effects of spatial distribution and the localization of mobile species in the composite, where there are two-phase distributions of ions in the bulk of the composite and ions in the double layer.

The similar shape of the CVs recorded at different scan rates (for all electrolytes) indicates excellent electrochemical reversibility of the PANI/PVA and PANI/Zr/PVA composites. As the scan rate was increased from 25 to 75 mV/s, the current response didn't change greatly. Some changes were observed only for PANI/PVA composite in 0.5 M H_2SO_4 (**Fig. 4e**). The highest current (0.08 A) is observed for PANI/Zr/PVA composite in 0.5M

NaCl and the lowest for PANI/Zr/PVA in 0.5 M H_2SO_4 and PANI/PVA composite in 0.5M NaCl.
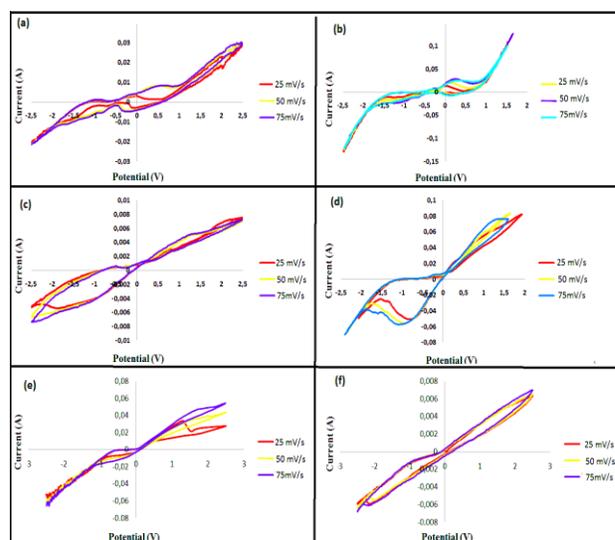

Fig. 4. Cyclic voltammograms of PANI/PVA composite in 0.5M KOH (a), 0.5 M NaCl, (c) 0.5 M H_2SO_4, (e) electrolytes and PANI/Zr/PVA composite in 0.5M KOH, (b) 0.5 M NaCl, (d) 0.5 M H_2SO_4 and (f) electrolytes at various voltage scan rates.

Also, **Fig. 4** shows that the width of electrochemical window depends on types of the composite and the electrolyte but not less than 2.5 V and more, than 5 V. It is very important property for energy storage technology.
Fig. 5 shows galvanostatic charge–discharge curves of the PANI/PVA and PANI/Zr/PVA composites at the currents of 0.5 mA, 1 mA, 2 mA and 3 mA as a function of time. The profiles show there is no proportionality between the increasing currents and the decreasing discharge times resulting in higher capacitances observed at lower discharge currents. Also, it is obvious that both composites are capable to store charge (the horizontal plots on the charge discharge curves).

The specific capacitance was calculated at different currents from the equation

$$Cs = \frac{I}{\frac{dV}{dt} \times m}$$

where, I – discharge current, A; dV/dt – potential changes; m – weight of the active material, g.

Table 1. Specific capacitance and charge-discharge times of PANI/PVA and PANI/Zr/PVA composites.

Current, mA	PANI/PVA								
	Type of electrolyte								
	0.5 M KOH			0.5 M NaCl			0.5 M H_2SO_4		
	Cs, F/g	t_c, s	t_d, s	Cs, F/g	t_c, s	t_d,s	Cs, F/g	t_c, s	t_d, s
0.5	161.3	225	520	56.2	170	1000	38.5	90	200
1	108.7	190	480	71.4	150	850	33.6	70	190
2	125	150	195	83.3	80	500	31.3	60	100
3	120.7	150	220	53.6	50	200	44.1	30	80
	PANI/Zr/PVA								
0.5	61.7	150	490	31.1	108	500	16.5	30	200
1	56.8	330	530	31.9	95	350	23.1	20	140
2	164	330	400	49.4	55	300	32.8	25	110
3	18.8	90	120	40.9	20	110	24.1	25	55

The calculation results are presented in **Table 1**. The specific capacitance strongly depends on the type of electrolyte. The highest values are attributed to 0.5M KOH and the lowest to 0.5M H_2SO_4 electrolyte. Also, influence of zirconium is obvious which expressed in total decrease

of specific capacitance in 0.5M NaCl and 0.5 M H_2SO_4. Specific capacitance of PANI/Zr/PVA composite in 0.5 KOH electrolytes dramatically decreased comparing to PANI/PVA at all currents excluding 2 mA when increasing of specific capacitance from 125 to 164 F/g is observed. Furthermore, *Cs* of PANI/Zr/PVA composite in 0.5M NaCl and H_2SO_4 slightly depends on the current value.
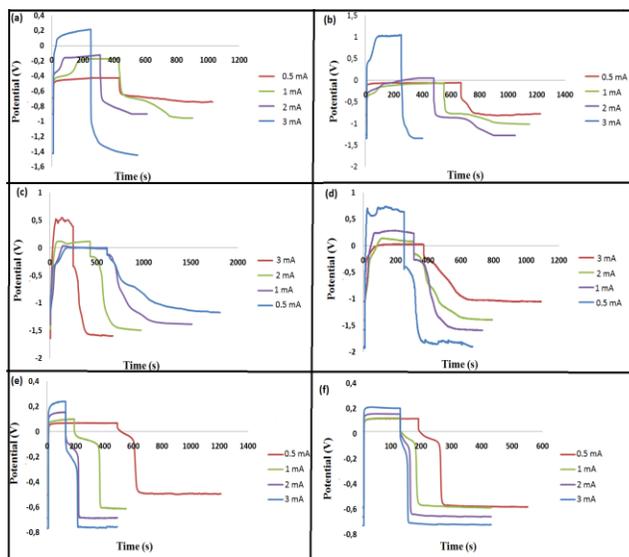

Fig. 5. Charge-discharge curves of PANI/PVA in 0.5M KOH (a), 0.5 M NaCl (c), 0.5 M H_2SO_4 (e) electrolytes and PANI/Zr/PVA in 0.5M KOH (b), 0.5 M NaCl (d), 0.5 M H_2SO_4 (f) electrolytes at different currents.

Conclusion

PANI and PANI/Zr composite powders were prepared by *in situ* polymerization of aniline using ammonium peroxodisulfate as an oxidizing agent. Synthesis of PANI was confirmed by UV-Vis spectroscopy. Strong chemical interaction between PANI and zirconium particles causes red shift of the absorption transition to higher wavelength. SEM images clearly showed the fiber-like structure both of PANI and PANI/Zr composite powders. BET investigations showed increasing of specific surface area with incorporation of zirconium particles to pristine PANI from 66.8 to 142.05 m^2/g. PANI and PANI/Zr composite powders were used for preparing PANI/PVA and PANI/Zr/PVA composites which were electrochemically characterized. The electrochemical supercapacitor measurements were performed in a 0.5M KOH, 0.5M NaCl and 0.5M H_2SO_4 electrolytes employing cyclic voltammetry and charge-discharge techniques in the galvanostatic mode. Shape of the CVs curves showed that electrochemical processes, including mixed electron-ionic controlled conductivity and redox-driven composition–structure relations proceed. Also, good electrochemical reversibility of prepared composites was demonstrated. The highest supercapacitance values were found to be 161.3 F/g for PANI/PVA composite in 0.5M KOH at 0.5 mA and 164 F/g for PANI/Zr/PVA composite in 0.5 M KOH at 2 mA. We expect the PANI/PVA and PANI/Zr/PVA composites have applications in new energy storage devices.

Reference

1. Gonçalves, G.S.; Baldissera, A.F.; Rodrigues Jr., L.F.; Martini, E.M.A.; Ferreira, C.A. ; *Synth. Met.*, **2011**, *161*, 313.
   DOI: 10.1016/j.synthmet.2010.11.043
2. Kazantseva, N.E. Magnetic Particle-Filled Polymer Microcomposites, In Polymer Composites; Thomas, S,; Kuruvilla, J.; Malhotra, S.K.; Goda, K.; Sreekala, M.S. A.P.F. (Eds.); Wiley-VCH, **2012**, pp.613.
   DOI: 10.1002/9783527645213
3. Wang, W.; Gumfekar, S.P.; Jiao, Q; Zhao, B.; *J. Mater. Chem. C.*, **2013**, *1* , 2851.
   DOI: 10.1039/C3TC00757
4. Hamzehie, M.E.; Samiee, L.; Fattahi, M.; Seifkordi, A.A.; Shoghi, F.; Maghsodi, A.; *Renewable Energy*, **2015**, *77*, 558.
   DOI: 10.1016/j.renene.2014.12.042
5. Shishov, M. A. 9tn biennial international workshop fullerenes and atomic clusters. Diagnostics of carbon nanostructures, **2009**.
6. Ivanova, V. T.; Katrukha, G.S.; Timofeeva, A. V.; Ilyna, M. V.; Kurochkina, Y. E.; Baratova , L.A.; Sapurina I. Yu.; Ivanov , V. F.; *Journal of Physics Conference Series*, **2011**.
   DOI: 10.1088/1742-6596/291/1/012004
7. Chen, P.Y.; Lee, C.P.; Vittal R*.; J. Power Sources*, **2010**, *195(12)*, 3933.
   DOI: 10.1016/j.jpowsour.2009.12.086
8. *Kim, J-Y.; Shin, D-H.; Ihn, K-J.; J. Appl. Polym. Sci.*, **2005**, *97(6)*, 2357.
   DOI: 10.1002/app.21807
9. M.; Moghimi, A.; Naderizadeh, B.; Maddah, B.; *Scientia Iranica*, **2011**, *18(6)*, 1327.
   DOI: 10.1016/j.scient.2011.08.013
10. Alam, M.; Ansari, A. A.; Shaik, M. R.; Alandis, N. M.; *J. Chem.*, **2013**, *6*, 341.
    DOI: 10.1016/j.arabjc.2012.04.021
11. Zhu, C-L.; Chou, S-W.; He, S-F.; Liao, W-N.; Chen, C-C.; *J. Nanotechnol.*, **2007**, *18(27)*, 1.
    DOI: 10.1088/0957-4484/18/27/275604
12. Zheng, L.; Xu Y.; Jin D.; Xie, Y.; *Chemistry - An Asian Journal*, **2011**, *6(6)*, 1505.
    DOI: 10.1002/asia.201000770
13. Srivastava, S.; Kumar, K.; Singh, V.N.; Singh, M.; Vijay, Y.K. *Int. J. Hydrogen Energy*, **2011**, *36(10)*, 6343.
    DOI: 10.1016/j.ijhydene.2011.01.141
14. Kunteppa, H.; Ameena Parveen; Harish Kumar, H. G.; Roy, A. S., *Adv. Mat. Lett.* **2013**, *4(11)*, 856.
    DOI: 10.5185/amlett.2013.3444
15. Araujoa, B.L.P.; Araujob, E.S.; Santosb, R.F.; Pachecoc, A.P.; *Microelectronics. J.,* **2005**, *36*, 1055.
    DOI: 10.1016/j.mejo.2005.04.024
16. D.S.; Shaikh, J.S.; Dalavi, D.S.; Kalagi, S.S.; Patil, P.S.; *Mater. Chem. Phys.*, **2011**, *128*, 449.
    DOI: 10.1016/j.matchemphys.2011.03.029
17. Liua, Q.; Nayfehb, O.; Nayfehb, M. H.; Yaua, S.; *Nano Energy*, **2013**, *2*, 133.
    DOI: 10.1016/j.nanoen.2012.08.007
18. Lin, H.; Li, L.; Ren, J.; Cai, Z.; Qiu, L.; Yang, Z.; Peng, H.; *Sci. Rep.*, **2013**.
    DOI: 10.1038/srep01353
19. Mohamoud, M.A., Ben Aoun, S., *J. of Taibah University for Science*, **2014***, 8*, 337.
    DOI: 10.1016/j. jtusci.2014.03.001